

Searches for ultra-high-energy photons with the Pierre Auger Observatory

Nicolás González^{a,b,c,*} for the Pierre Auger Collaboration^d

^a*Università degli studi di Torino (UniTo), via Pietro Giuria 1, 10125, Turin, Italy*

^b*Istituto Nazionale di Fisica Nucleare (INFN), Sezione di Torino,
via Pietro Giuria 1, 10125, Turin, Italy*

^c*Instituto de Tecnologías en Detección y Astropartículas (ITeDA),
Av. Gral Paz 1499, B1650KNA San Martín, Buenos Aires, Argentina*

^d*Observatorio Pierre Auger, Av. San Martín Norte 304, 5613 Malargüe, Argentina*
Full author list: https://www.auger.org/archive/authors_2024_11.html

E-mail: spokespersons@auger.org

Ultra-high-energy (UHE, $E \gtrsim 10^{17}$ eV) photons are expected to originate from the interaction of UHE cosmic rays with background radiation fields, as well as from more exotic processes like the decay of hypothetical super-heavy dark matter particles. UHE photons produced at cosmic-ray sources are key ingredients for enhancing our multimessenger understanding of the cosmic-ray acceleration and transient phenomena. Pierre Auger Observatory, designed to investigate UHE cosmic rays, offers unparalleled sensitivity to UHE photons. In this contribution, we present recent results of photon searches above $10^{16.7}$ eV obtained with data collected prior to the upgrade of the Observatory. Additionally, we discuss directional and follow-up searches conducted in coincidence with gravitational wave events detected by LIGO/Virgo, highlighting the role of the Observatory in advancing multi-messenger astronomy at the highest energies.

*7th International Symposium on Ultra High Energy Cosmic Rays (UHECR2024)
17-21 November 2024
Malargüe, Mendoza, Argentina*

*Speaker

1. Introduction

The origin and the acceleration of ultra-high-energy (UHE, $E \gtrsim 10^{17}$ eV) cosmic rays remain elusive. They can be investigated by detecting photons produced through cosmic-ray interactions with surrounding matter or radiation near the sources [1]. Photons with energies between 10^{14} eV and 10^{18} eV interact with background radiation fields, limiting their travel to a few Mpc. This makes them excellent probes for studying Galactic sources [2].

In addition to astrophysical sources, cosmogenic photons are expected to arise from interactions between UHE cosmic rays and the cosmic microwave background, as well as the extragalactic background light, in intergalactic space [3–5]. Lighter nuclei produce more secondary photons due to their higher interaction rates with background photons. Consequently, detecting UHE photons provides constraints on cosmic-ray sources, their composition, and acceleration mechanisms. Interactions between UHE cosmic rays and Galactic disk matter significantly contribute to the cosmogenic photon flux through neutral pion decay [6]. Similar to fluxes from UHE cosmic-ray propagation, this component depends on the cosmic-ray flux and composition, the distribution of the gas in the Galactic disk, and the interaction cross-sections.

The decay of super-heavy dark matter (SHDM) within the Galactic center may be a substantial contribution to the diffuse photon flux above 10^{16} eV [7, 8]. Since the photon flux generated in the Galactic center is not significantly attenuated owing to the source proximity, the Galactic center is a prime candidate for probing gamma-ray production from SHDM decay channels [9, 10].

The flux of UHE photons is expected to be several orders of magnitude lower than that of cosmic rays. Distinguishing photons from the overwhelming background of charged cosmic rays is challenging. Both cosmic rays and photons initiate air showers — cascades of secondary particles in the atmosphere — and the separation is based on air-shower properties: showers initiated by photon primaries develop almost entirely through electromagnetic processes, whereas those initiated by hadrons contain significantly more muons. Due to the lower multiplicity of electromagnetic compared to hadronic interactions, the atmospheric depth of the maximum shower development, X_{\max} , is deeper for photons than for hadronic primaries. Furthermore, the reduced muonic component in photon-induced showers leads to a steeper lateral spread of the shower and a slower signal rise in ground-based detectors compared to hadronic showers. These features form the basis for photon identification in data collected by the Pierre Auger Observatory.

The Pierre Auger Observatory [11] integrates multiple detection techniques to extract information from the air showers, employing a surface detector (SD) to sample particles at the ground, a fluorescence detector (FD) to observe the emitted light during the shower’s development, and an underground muon detector (UMD) to measure high-energy muons from the air showers. The SD comprises 1660 water-Cherenkov detectors arranged in three a triangular grids with spacings of 1500 m (SD-1500), 750 m (SD-750) and 433 m (SD-433). The FD is composed of 27 telescopes across four sites overlooking the SD. The UMD is composed of buried scintillation modules alongside the SD stations of the SD-750 and SD-433 [12]. With an instrumented area of 3000 km^2 , the Pierre Auger Observatory achieves an unparalleled exposure to photons above 5×10^{16} eV [13].

In this contribution, we summarize the UHE photon searches conducted at the Pierre Auger Observatory. We report integral upper limits on the diffuse fluxes above 5×10^{16} eV in [Sec. 2](#) and discuss the sensitivity to steady and transient sources in [Sec. 3](#), before concluding in [Sec. 4](#).

2. Diffuse searches

The complementary detection techniques of the Pierre Auger Observatory can be employed to measure the distinctive features of photon-initiated showers. The measured observables are combined into a single discriminator using a multi-variate method, such as Boosted Decision Trees (BDT). Given that no UHE photons have yet been detected, the expected distribution of the discriminator in the case of photon events is built from dedicated detector simulations [14]. To classify an event as a photon candidate, the associated value of the discriminator is compared to the photon candidate cut, which is chosen at the median of the photon distribution. Thus, the signal efficiency is fixed by definition at 50%. Complementarily, the background contamination is the fraction of hadron-initiated events misclassified as photon candidates within the dataset.

Four discrimination methods, optimized in different energy ranges, are applied to the recorded data to search for unresolved, direction-independent photon fluxes, as discussed in the following.

2.1 Photon-hadron discrimination methods

The SD-433 is employed to detect air showers in the energy range above 5×10^{16} eV [15], providing information on the primary energy and shower geometry. The photon-hadron discrimination method relies on the measurement of the muon component of the air showers by the UMD. For each event, the muon densities measured at various distances from the shower axis are combined into a discrimination observable [16]. The background contamination ranges between 10^{-4} to 10^{-7} under the assumption of a pure-proton background, a conservative one in light of the deficit of muons identified in the air-shower simulations [17]. Applying the photon candidate cut to ~ 15 months of data (equivalent to an exposure of $\sim 0.6 \text{ km}^2 \cdot \text{sr} \cdot \text{yr}$) yielded no photon candidate events.

The hybrid data recorded by the SD-750 and the FD are exploited to discriminate a photon signal among the hadronic background above 2×10^{17} eV [18]. For this task, the direct measurements of X_{max} are complemented by the convolution of the measured SD signals in each event [19]. The footprint size, represented by the number of triggered stations per event, is also considered. To combine the three observables, a BDT method was trained using simulated proton events as background. Although a background contamination of two events was expected, no photon candidate events were detected in the search data set spanning 5.5 yr or $\sim 2.5 \text{ km}^2 \cdot \text{sr} \cdot \text{yr}$.

Above 10^{18} eV, the observables employed are X_{max} and a proxy for the muon content extracted from the signals acquired by stations of the SD-1500 [20], calculated by matching the measured signals to a decomposition between electromagnetic and muon components within the air-shower Universality framework [21]. The two observables are combined by means of a Fisher discriminant. In the data set taken over 12 yr, or $\sim 1000 \text{ km}^2 \cdot \text{sr} \cdot \text{yr}$, 22 photon candidate events were found [22]. This number is consistent with the expected background contamination of 30 ± 15 .

The search for UHE photons above 10^{19} eV is conducted with data acquired by the SD-1500. The discrimination strategy is based on comparing the measured SD signals and their risetime to the average expectation in data [23]. The two observables are combined into a Fisher discriminant. The searched data set collected over 16 yr has an exposure of $\sim 17,000 \text{ km}^2 \cdot \text{sr} \cdot \text{yr}$. Although 16 candidate events were found, this number is compatible with the background contamination estimated with a subset of data, hence free from assumptions about the cosmic-ray composition.

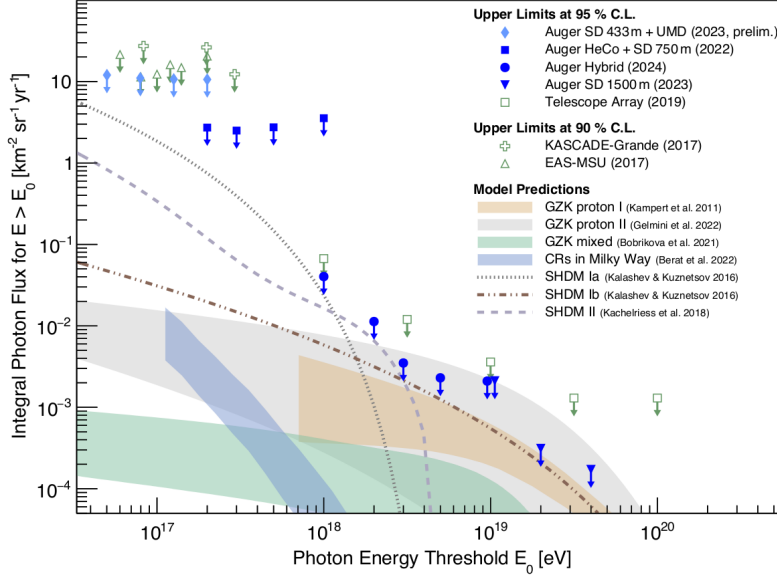


Figure 1: The current upper limits on the integral photon flux established by the four searches described in this article (solid markers). The upper limits published by other experiments are shown as empty markers. Filled bands indicate predicted cosmogenic photon flux ranges for varying cosmic-ray compositions. Dashed lines indicate SHDM flux predictions under different theoretical scenarios [25].

2.2 Upper limits to the diffuse photon flux

From the absence of photon events, upper limits on the integral photon flux were calculated. These limits are inversely proportional to the exposure of the detection systems, which accounts for both the operational uptime of the detectors and the efficiency in detecting photon events.

As illustrated in Fig. 1, the upper limits derived with the data collected by the Pierre Auger Observatory set stringent constraints on UHE photon fluxes across four decades in energy above 5×10^{16} eV. The cosmogenic fluxes from UHE cosmic-ray propagation, represented by the colored bands, are within reach above 10^{18} eV. The component due to UHE cosmic rays in the Galaxy, which may be predominant below 10^{17} eV, is around two orders of magnitude below the current sensitivity. The current photon searches can be improved from the constant increase in exposure over time, with which the upper limits scale inversely, from the application of more advanced analysis techniques, and from the ongoing detector upgrade of the Pierre Auger Observatory (see Sec. 4). It will be possible to also reach the predictions from the decay of SHDM [8] (dashed grey and purple lines), thus constraining the phase space of mass, lifetime and decay channels of these particles [24].

The searches for diffuse photon fluxes are space- and time-integrated by definition. An increased sensitivity can be achieved when focusing on certain directions of the sky housing catalogued gamma-ray sources or in coincidence with a detection of a significant astrophysical event, as discussed in the next section.

3. Directional searches

The hybrid data of the Pierre Auger Observatory, with angular resolution of $\sim 0.7^\circ$ above 2×10^{17} eV, enable point-like photon source searches. Target sources of UHE photons contain Galactic objects, as well as some nearby extragalactic ones, namely three powerful gamma-ray emitters in the Large Magellanic Cloud and the core region of Centaurus A [26].

3.1 Steady point-like sources

A blind search was conducted to identify an excess of photon-like events from any direction in the sky [27]. Using hybrid data acquired between January 2005 to September 2011 with the SD-1500 and the FD between 2×10^{17} eV and 3×10^{18} eV, photon-like events are selected using a BDT method trained with five composition-sensitive observables. Photon candidates are selected through a cut in the discriminator optimized for each direction. Averaged over all target directions, the signal efficiency is 81.4% with a background contamination of 4.8%. No point source of UHE photons was identified and upper limits on the directional photon flux were placed, as shown in Fig. 2, left.

To minimize the statistical penalty of an all-sky search, catalogued candidate sources were grouped into 12 classes [26]. This targeted search follows the same rationale as the blind search, although with a larger dataset from January 2005 to December 2013. No statistical excess of photon-like events is found, and upper limits are given for each class. A source class of specific interest is the Galactic center for which the H.E.S.S. Collaboration measured a gamma-ray flux up to about 5×10^{13} eV without any observation of a cutoff or a spectral break [28]. Upper limits have been set around 10^{18} eV in the direction of the Galactic center, as represented by the green line in Fig. 2, right. Such a constraint is compatible with an extrapolation of the measured gamma-ray spectrum with a cutoff energy at 2×10^{18} eV.

3.2 Transient sources

While steady sources provide time-integrated constraints, transient sources present unique opportunities for detection, as they are often associated with high-energy astrophysical events that may escape steady-source searches. In this regard, Pierre Auger Collaboration contributes to the global multimessenger effort by conducting follow-up UHE photon searches associated with gravitational wave (GW) events [29].

In order to maintain a high sensitivity towards a possible photon signal from a transient source despite the considerable background, a dedicated GW selection strategy has been developed. Four classes of accepted GW events are defined in Fig. 3, left, in the space of the 50%-sky localization region, $\Omega_{50\%}$, and luminosity distance, D_L . Sources closer than 50 Mpc (classes III and IV) are the most promising candidates to yield a detectable flux of UHE photons, accounting for the attenuation due to interactions with background radiation fields. On the contrary, the detection of a photon in coincidence with a well localized source located further than 180 Mpc (classes I and II) would give a strong hint towards new physics, since the universe on large scales is opaque to UHE photons in the framework of standard model interactions.

Under these criteria, 23 GW events from the three GW catalogs published by LIGO/Virgo qualified to the follow-up. Out of these 23 GW events, only ten had at least partial overlap with the

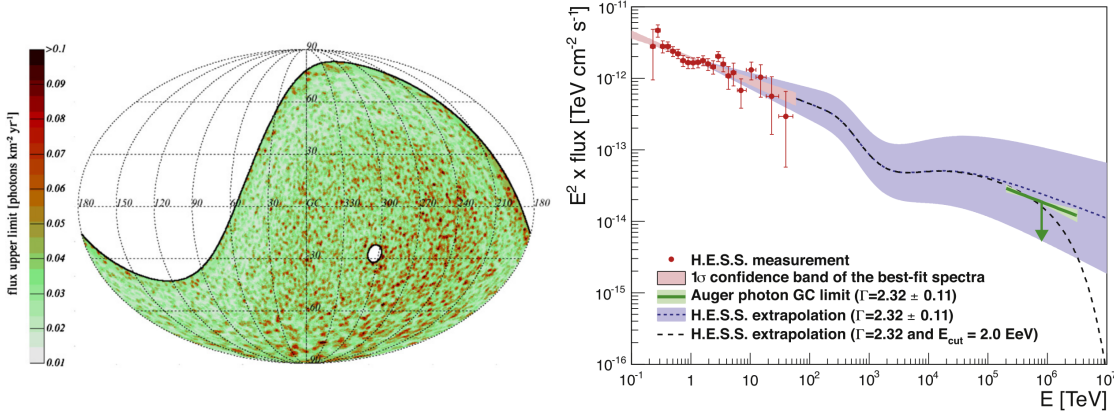


Figure 2: Left: The upper limits to the photon flux at 95% confidence level in Galactic coordinates in a blind all-sky search [27]. Right: The upper limits on the photon flux from the Galactic center obtained with data collected by the Pierre Auger observatory (green line) [26] together with the measured spectra reported by the H.E.S.S. collaboration (red markers) [28]. The measured photon flux is extrapolated into UHE with and without a cutoff energy (dashed lines), given the quoted spectral index and its uncertainties (blue shaded region).

field of view of the SD in either of the two considered time windows, i.e., ± 500 s around the time of the GW and +1 day after.

Photon candidates are identified using the method designed for the diffuse photon search above 10^{19} eV. No photon candidate events have been observed for any of the ten GW events studied in the respective time windows. Upper limits on the photon emission from GWs at UHE were placed for the first time [29], particularly for seven of them in a 1-day time window as displayed in Fig. 3, right. Upper limits on UHE photon fluence are ~ 7 MeV cm $^{-2}$ (short time window) and ~ 35 MeV cm $^{-2}$ (long time window).

Among the seven GW events followed up in the 1-day time window is the binary neutron star (BNS) merger event GW170817 [30]. Due to its proximity, the upper limit on the flux of UHE photons from this source above 4×10^{19} eV can be translated into an upper limit of 20% on the energy transferred from the GW into UHE photons.

4. Summary and outlook

The Pierre Auger Observatory collected an unrivaled exposure to UHE photons above 5×10^{16} eV and its data have been employed to set the most stringent upper limits to the diffuse photon flux across four decades in energy. The stringent upper limits on photon fluxes constrain models of SHDM decay and provide insights into the composition and acceleration mechanisms of cosmic rays.

The SD-1500 has enough exposure to study steady point sources with nearly full sky coverage. No significant deviations from background expectations were found in searches for point-like UHE photon sources. Flux upper limits from photon point sources constrain the extrapolation of measured TeV fluxes to UHE, as discussed for the particular case of the Galactic center.

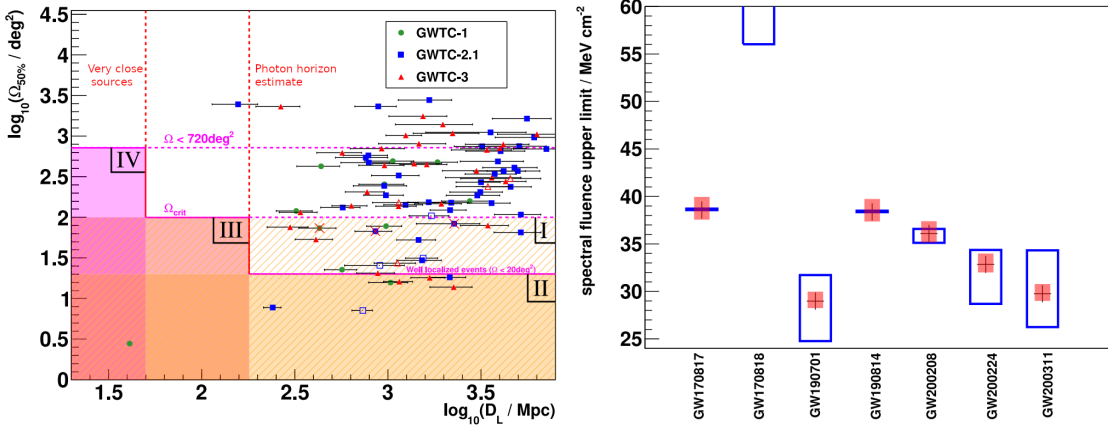


Figure 3: Left: The three classes of selected GW sources for the UHE photon follow-up search as defined by their 50%-localization region, $\Omega_{50\%}$, and luminosity distance, D_L . Figure edited from [29]. Right: Upper limits on the spectral fluence of UHE photons from the selected GW sources during one sidereal day after the GW detection. The empty blue and shaded red bars correspond to the variation of the upper limits due to the directional uncertainty of the source and the impact of a variation of the spectral index (between -2.3 and -1.7), respectively. The central value in the case of GW170818 is outside the displayed axis range and the blue bar has no upper bound since the localization region of GW170818 leaks outside the declination band accessible to the SD [29].

A possible outflow of UHE photons from the GW sources detected in recent years have been investigated. The absence of coincident photon signals enabled the derivation of the first upper limits on the flux of photons from GW sources. The limit on the BNS merger GW170817 adds one further piece to the overall multimessenger puzzle by constraining the electromagnetic outflow of the source in the UHE regime.

The Pierre Auger Observatory has been upgraded to enhance the air-shower component separation [31]. The upgrade comprises the installation of plastic scintillation detectors on top of each SD station, faster readout electronics and a larger dynamic range of the WCD to measure high particle densities closer to the shower core. Moreover, the SD-750 and SD-433 are being furnished with an extended deployment of UMD stations. Lastly, radio antennas are being installed next to each SD station to provide improved shower information for inclined air showers. The upgrade positions the Pierre Auger Observatory to achieve unprecedented sensitivity to UHE photons, potentially leading to their first unambiguous detection and solidifying its role as a multi-messenger observatory in the coming decade.

References

- [1] M. Niechciol et al. [Pierre Auger Coll.], *Universe* **8** (2022) 579.
- [2] Z. Cao et al., [LHAASO Coll.], *Nature* **594** (2011) 33-36.
- [3] G. Gelmini, O. Kalashev and D. Semikoz, *Universe* **8** (2022) 402.
- [4] A. Bobrikova et al., *PoS* **395** (2021) 449.
- [5] R. Alves Batista et al., *J. Cosmol. Astropart. Phys.* **01** (2019) 002.
- [6] C. Bérat et al., *Astrophys. J.* **929** (2022) 55.
- [7] P. Abreu et al. [Pierre Auger Coll.], *Phys. Rev. D* **107** (2023) 042002.

- [8] L. Anchordoqui et al., *Astropart. Phys.* **132** (2021) 102614.
- [9] R. Aloisio et al. [Pierre Auger Coll.], these proceedings.
- [10] O. Deligny, these proceedings.
- [11] A. Aab et al. [Pierre Auger Coll.], *Nucl. Instrum. Meth. D* **798** (2015) 172-213.
- [12] J. de Jesús et al. [Pierre Auger Coll.], *PoS* **444** (2023) 267.
- [13] F. Salamida et al. [Pierre Auger Coll.], *PoS* **444** (2023) 016.
- [14] E. Santos et al. [Pierre Auger Coll.], *PoS* **444** (2023) 248.
- [15] G. Bricchetto et al. [Pierre Auger Coll.], *PoS* **444** (2023) 398.
- [16] N. González et al. [Pierre Auger Coll.], *PoS* **444** (2023) 238.
- [17] K. Almeida Cheminant et al., these proceedings.
- [18] P. Abreu et al. [Pierre Auger Coll.], *Astrophys. J.* **933** (2022) 125.
- [19] G. Ros et al., *Astropart. Phys.* **47** (2013) 10-17.
- [20] P. Savina, C. Bleve, and L. Perrone, *PoS* **358** (2019) 414 .
- [21] M. Ave, M. Roth, and A. Schulz, *Astropart. Phys.* **88** (2017) 46-59.
- [22] A. Abdul Halim et al. [Pierre Auger Coll.], *Phys. Rev. D* **110** (2024) 062005.
- [23] P. Abreu et al. [Pierre Auger Coll.], *J. Cosmol. Astropart. Phys.* **05** (2023) 021.
- [24] M. Kachelriess, O. Kalashev and M. Kuznetsov, *Phys. Rev. D* **98** (2018) 083016.
- [25] M. Niechciol et al. [Pierre Auger Coll.], In Proceedings of *45th COSPAR Conference*, July 13-21, 2024, Busan, Korea.
- [26] A. Aab et al. [Pierre Auger Coll.], *Astrophys. J. Lett.* **837** (2017) 25.
- [27] A. Aab et al. [Pierre Auger Coll.], *Astrophys. J.* **789** (2014) 160.
- [28] A. Abramowski et al. [H.E.S.S. Coll.], *Nature* **531** (2016) 476-479.
- [29] A. Abdul Halim et al. [Pierre Auger Coll.], *Astrophys. J.* **952** (2023) 91.
- [30] B. Abbott et al. [Pierre Auger Coll. et al.], *Astrophys. J. Lett.* **848** (2017) 12.
- [31] D. Schmidt, these proceedings.